Pergamon

0301-9322(93)E0032-Z

Int. J. Multiphase Flow Vol. 20, No. 4, pp. 763–773, 1994

0301-9322/94 $7.00 + 0.00

DEVELOPMENT OF A MICROWAVE PLASMA-FLUIDIZED BED REACTOR FOR NOVEL PARTICLE PROCESSING

M. MATSUKATA[1], K. SUZUKI[1], K. UEYAMA[1] and T. KOJIMA[2]

[1]Department of Chemical Engineering, Faculty of Engineering Science, Osaka University, 1-1 Machikaneyama-cho, Toyonaka-shi, Osaka 560, Japan

[2]Department of Industrial Chemistry, Faculty of Engineering, Seikei University, 3-3-1 Kichijojikita-machi, Musashino-shi, Tokyo 180, Japan

(Received 23 May 1993; in revised form 13 December 1993)

Abstract—We developed a fluidized bed–chemical vapor deposition (CVD) reactor for a novel method of particle processing, such as particle coating and surface treatment. Microwave plasma was applied as an excitation source of reactive gases, and alumina and silicon were used as bed materials. The hydrodynamic behavior of the plasma-bubbling fluidized bed was studied and the field of plasma generation was investigated optically. Only minor plasma generation was noted in the dense phase. Plasma emission was observed in most of the bubbles in the alumina-fluidized bed, while plasma generated at the surface of the silicon-fluidized bed where bubbles splashed. Methane conversion was carried out in the alumina-fluidized bed as a model reaction. Although excitation of methane occurred in bubbles, excited species entered into the dense phase from bubbles and were effectively converted to carbon on the surface of the particles. Thus, heterogenous CVD on the surface of particles may occur in this reactor.

Key Words: microwave plasma, fluidized bed, particle processing, chemical vapor deposition

1. INTRODUCTION

The plasma state has been used extensively in chemical vapor deposition (CVD) to make thin films on flat surfaces at low pressures. The use of plasma in CVD processing allows excited species to form easily, and this feature of plasma may be applicable to particle processing, such as coating. Particle behavior in plasma has been investigated in coal gasification, roasting and decarbonization. In most plasma reactor studies, dilute systems were used in which particles were continuously injected into a plasma jet. In such designs, particles must remain in plasma and be in uniform contact with excited species in order to achieve CVD on the particles.

Recently, several types of fluidized bed reactors have been proposed. Jurewicz *et al.* (1985) first proposed the use of fluidizing phenomena for particles using a d.c. plasma for particle processing. Flamant (1989) developed a d.c. plasma-spouted bed reactor in which a d.c. plasma jet penetrated the particle bed, and reported on the hydrodynamics and heat transfer in the bed. Kojima *et al.* (1991) and Matsukata *et al.* (1992) have developed a d.c. plasma-jetting fluidized bed reactor for particle processing, and applied their design to methane conversion. Heterogeneous decomposition of methane giving carbonaceous deposits on alumina surface was observed in and around the plasma jet. This suggested the possibility of CVD on particles in a plasma-fluidizing bed reactor. These reactors provided a stable plasma state and could be operated at around atmospheric pressure, thereby decreasing operating costs. However, the residence time of particles in the plasma jet was short and a long reaction time was needed to obtain sufficient deposits. Additionally, the sputtering of electrodes caused inevitable contamination. These are clearly drawbacks in applying a jetting fluidized bed to CVD processing.

The plasma state can alternatively be created using microwaves. Generally, microwaves generate a clean plasma that can be formed in a wide field. However, the field should be kept at pressures below about 100 Torr. A longer residence time of particles is expected in microwave plasma than in a d.c. plasma-fluidized bed provided the microwave plasma is stably formed in a fluidized bed. Wierenga & Morin (1989) and Rogers & Morin (1991) have developed a microwave plasma-fluidized bed and reported on its hydrodynamic behavior. They employed glass spheres with

diameters of 0.17–1 mm as bed material and confirmed that microwave plasma formed in the fluidized bed.

In the present study, we investigated the hydrodynamic behavior of a microwave plasma-bubbling fluidized bed using alumina and silicon particles as bed materials. In particular, the possibility of CVD processing in this type of reactor was explored since, to our knowledge, there are no reports of chemical reactions in such a reactor. We monitored the generation and breakdown of plasma in the bed using optical observations of plasma emission. Methane conversion was also carried out as a model reaction to explore the effect of bed materials on the progress of chemical reactions and to determine whether heterogeneous decomposition takes place on the surface of bed materials.

2. EXPERIMENTAL

Apparatus

Figure 1 schematically shows the experimental apparatus consisting of two parts: (1) the power circuit and (2) the gas-handling and reactor system. A microwave generator (Shin-nihon Musen Co., Ltd.) delivered 2.45 GHz microwaves at 0–1000 W. Plasma was generated at 200 W in all experiments. The microwave signal was transmitted through a series of waveguides including a power meter and tuning equipment, and was coupled to a resonance cavity. Four kinds of gases, Ar, H_2, CH_4 and He were used, and their flow rates were controlled with mass flow control valves and were measured using thermal mass flow sensors.

Figure 2 illustrates the fluidized bed reactor used in the present study. A quartz tube (i.d., 30 mm) was placed vertically in the resonance cavity and a porous plate made of quartz was set in the tube as a gas distributor. The absolute pressure corresponding to the reaction pressure was monitored at the top of the reactor, and the measured pressure was considered to be the same as that at the surface of the bed.

Hydrodynamic behavior

Fluidizing properties were studied by measuring pressure drop through the bed. Differential pressure was measured between two pressure sensors placed above the freeboard and below the distributor plate. Alumina and polycrystalline silicon were chosen as bed materials, both of which had an average particle diameter of 1.5×10^2 μm. Fluidization of each type of particle was carried out at 30 Torr under both plasmatic and non-plasmatic conditions. No appreciable difference was observed when fluidization was carried out at 15 Torr. Ar and H_2 were used as plasma gases.

Optical observations

Plasma emission was observed using optical fibers to confirm the generation of plasma in the fluidized bed. Optical fibers made of quartz were placed outside the reactor tube to observe any light emitted from the bed. The signal from the reactor was guided through the fibers to a photomultiplier and time variation in its intensity was recorded.

Methane conversion

Conversion of CH_4 was carried out under plasmatic conditions in the presence of bed particles. The feed gas comprised of 40% Ar, 10% CH_4, 40% H_2 and 10% He. Effluent gas was sampled at the outlet of the gas-handling system. Two gas chromatographs (Shimazu) with thermal conductivity detectors (TCD) and flame ionization detectors (FID) were used for determining gas composition. The reaction products of the CH_4 conversion were comprised mainly of C_2H_2, carbonaceous deposits (C), H_2 and unreacted CH_4. Trace amounts of C_2H_4 and C_2H_6 were formed. Since gas volume changed as CH_4 conversion progressed, helium was used as a reference to correct the change in gas volume in order to identify CH_4 and H_2 from the chromatogram using TCD. The chromatogram detected by the FID was used to obtain the molar ratio of C_2H_2 to CH_4. The molar flow rate of C_2H_2 was determined using that of CH_4 calculated from the chromatogram using TCD. The yield of carbon deposits was indirectly determined from the carbon balance.

3. RESULTS AND DISCUSSION

Fluidization phenomena

In an attempt to characterize the fluidization phenomena of the plasma-fluidized bed at reduced pressures, pressure drops through the bed were measured at various superficial velocities under plasmatic and non-plasmatic conditions. Figure 3 shows the experimental results for the fluidization of alumina and silicon at 30 Torr under the non-plasmatic condition. The plotted data were determined by subtracting the pressure drop caused by the distributor plate under the non-plasmatic condition from the measured pressure drop at a given superficial velocity. Horizontal solid lines represent the pressure drop, ΔP, calculated according to

$$\Delta P = 4mg/\pi D^2. \quad [1]$$

where

ΔP = pressure drop (Pa)
m = amount of particles packed (kg)
g = gravitational acceleration (m s^{-2})
D = inner diameter of reactor (m).

All experimental data in the fluidizing region were consistent with ΔP as calculated by [1]. The minimum fluidization velocities, U_{mf}, for Ar and H_2 were in good agreement with the values obtained from the equation by Wen & Yu,

$$U_{mf} = d_p^2(\rho_s - \rho_G)g/(1650\,\mu)(\mathrm{Re} < 20) \quad [2]$$

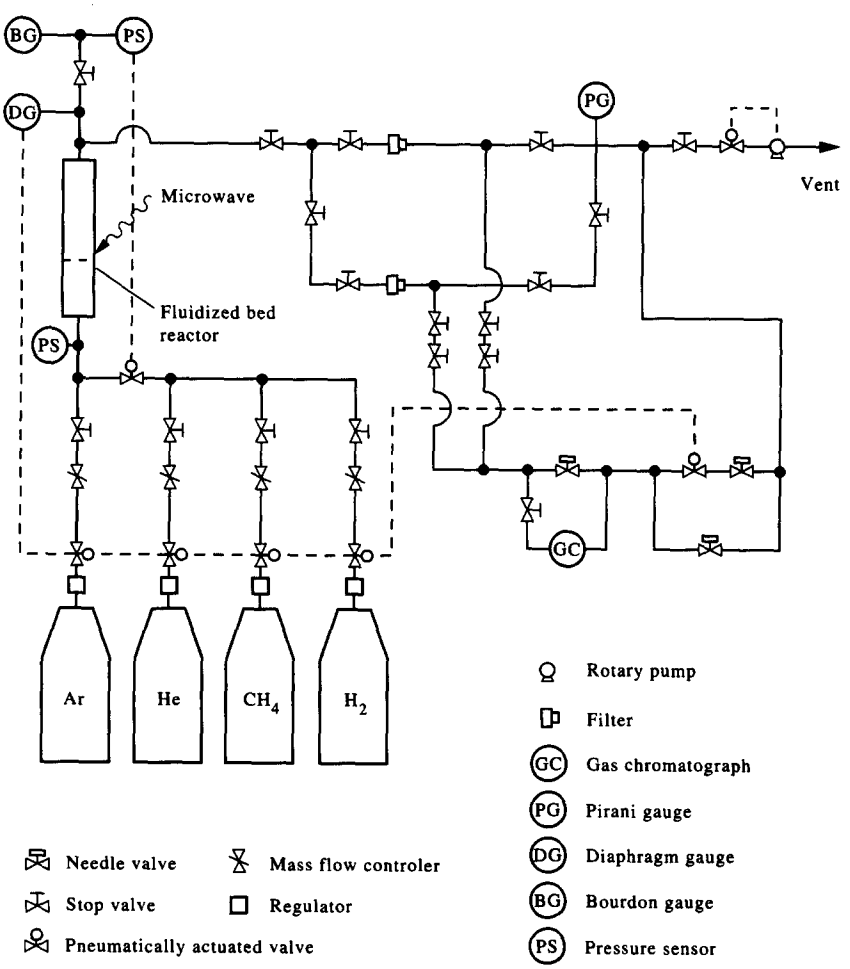

Figure 1. Schematic diagram of the experimental apparatus.

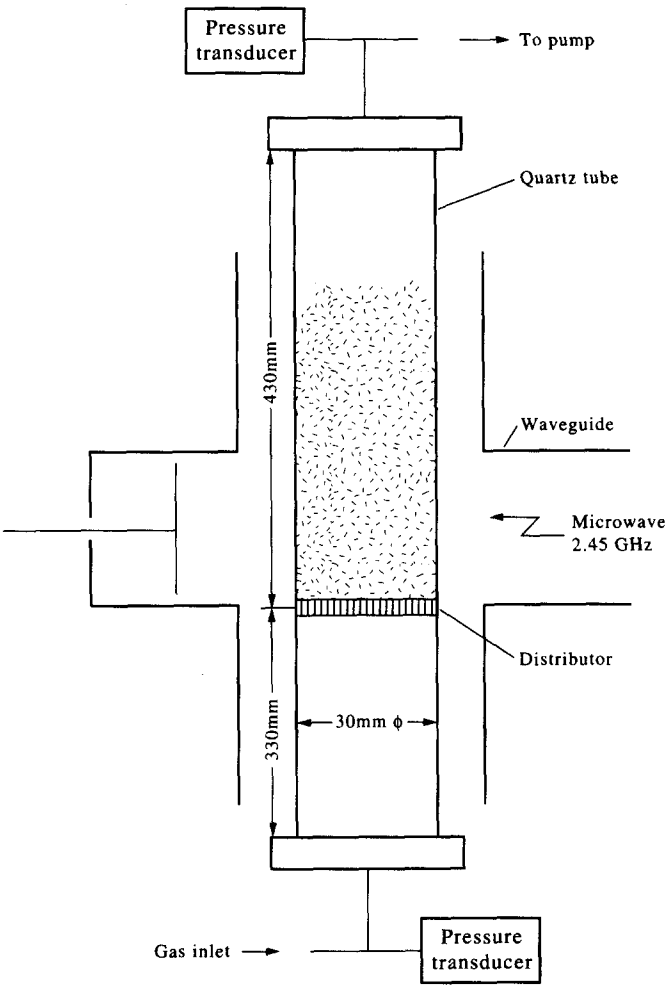

Figure 2. Microwave plasma-fluidized bed reactor.

where

U_{mf} = minimum fluidization velocity (m s^{-1})
d_p = average particle diameter (m)
ρ_s = density of solid (kg m^{-3})
ρ_G = density of gas (kg m^{-3})
μ = viscosity of gas (Pa s).

Re represents the Reynolds number and was less than 10^{-2} under the experimental conditions used. U_{mf} calculated according to [2] was 1.8×10^{-2} m s^{-1} for the alumina–Ar system, 4.7×10^{-2} m s^{-1} for the alumina–H_2 system, 1.4×10^{-2} m s^{-1} for the silicon–Ar system and 3.5×10^{-2} m s^{-1} for the silicon–H_2 system at 293 K. These values also agreed well with the experimental results. Thus, it is reasonable to consider that [1] and [2] hold for the particles and operational conditions employed in the present study.

Figure 3 shows the pressure drops measured under the plasmatic conditions. No plasma generation was observed in the four systems at low gas velocities forming a fixed bed of particles. Plasma emission was observed in the fluidized bed, while emission did not occur in the whole of the reactor. We visually observed mass-like plasma above the distributor plate, which, in the alumina-fluidized bed, ascended toward the surface of the bed. It appeared that plasma generated in bubbles and did not form in the dense phase. The plasma emission in the silicon-fluidized bed behaved differently; the interval between emissions was longer than in the alumina-fluidized bed. The phenomena of plasma emission in the fluidized bed will be discussed in detail below.

It should be noted that fluidization occurred at velocities less than U_{mf} calculated according to [2] for the alumina–Ar system [figure 3(a)]. Only the occurrence of electrophoresis could explain a pressure drop other than that caused by a thermal effect. Rogers & Morin (1990) discussed this electrophoretic effect on pressure drop through the bed and concluded that pressure drops associated with the electrophoretic effect are of the order of 10^{-1} Torr and below. Thus, the profile of pressure drop under the plasmatic condition is best understood in terms of a thermal effect. Measurement of the bed temperature under the plasmatic condition was difficult using the inserted thermocouples because the microwaves interacted with the thermocouples and interfered with the measurement system. The bed temperature was monitored by thermocouples in contact with the outer surface of the reactor. The measured temperature, which was believed to be close to that of the bed particles, was 360 ± 10 K for the alumina-fluidized bed and 380 ± 30 K for the silicon-fluidized bed. Judging from [2], the viscosity of the gas, μ, is the most important parameter governing U_{mf} under the plasmatic condition. The measured bed temperature did not explain the decrease in U_{mf} because μ at 400 K is about 1.2 times that at room temperature. Thus, the temperature of the gas was higher than that of the particles since some plasma was present in the fluidized bed, leading to an increase in μ. As a result, fluidization under the plasmatic condition was considered to be kept at gas velocities smaller than the calculated U_{mf}.

The pressure drops shown in figure 3(a) tended to be greater than those predicted by [1]; and [1] cannot explain this deviation in pressure drop through the particle layer under the fluidizing condition. Frequent plasma emission was observed around the plate and, consequently, μ of Ar was expected to increase there. Thus, the deviation to greater pressure drops was probably due to an increase in the pressure drop through the distributor plate. No decrease in U_{mf} in the presence of plasma was observed in the silicon–Ar system, as shown in figure 3(b), although anomalous deviation in pressure drop was observed.

Unlike the condition using Ar, experimental data obtained under the plasmatic condition using H_2 were nearly identical to those obtained under the non-plasmatic condition, as shown in figures 3(c) and (d). Visual observations indicated that stable H_2 plasma was difficult to generate in the

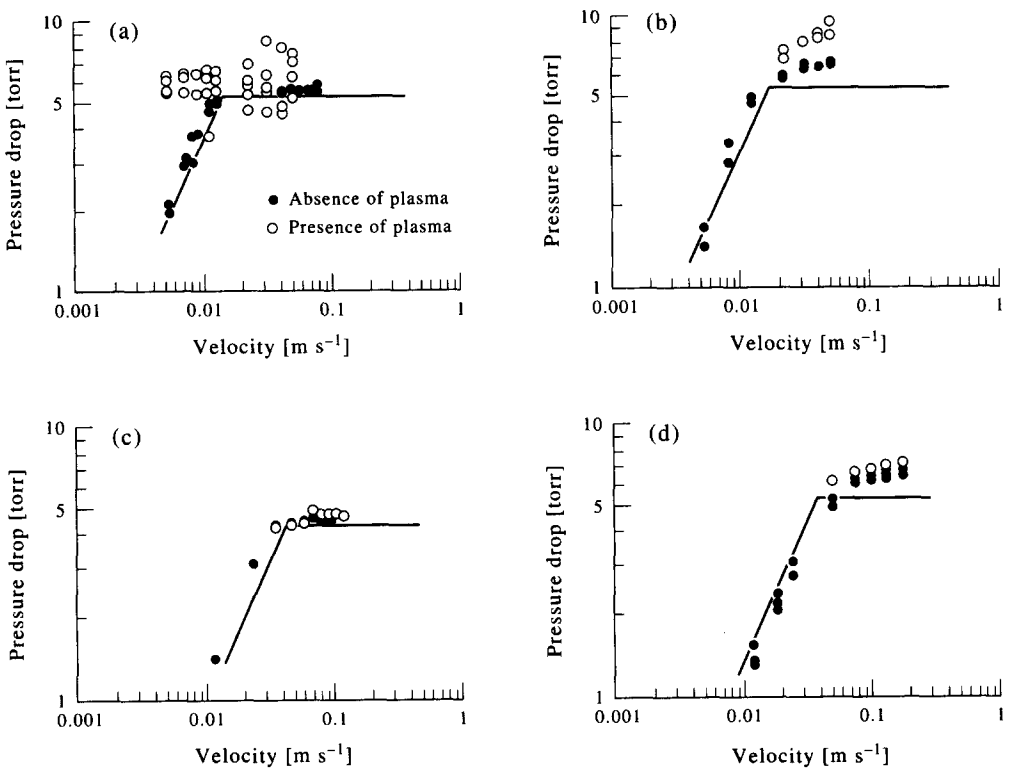

Figure 3. Comparison of pressure drop profiles for the absence and presence of microwave plasma. Particles: alumina, (a, b); silicon, (c, d). Gas: Ar, (a, c); H_2, (b, d). Horizontal solid lines were calculated by [1].

fluidized bed, which may be attributable to a smaller (ϵ_r)-1 value, 517.2×10^{-6}, for Ar, compared with 253.8×10^{-6} for H_2. It is likely that the instability of the H_2 plasma state made it difficult to increase the practical gas temperature.

Wierenga & Morin (1989) and Rogers & Morin (1991) reported different results from those described above. They employed glass spheres with diameters of 0.175–1 mm and reported that Ar plasma was generated even in a fixed bed. In the present study, generation of plasma was never observed when particles formed a fixed bed at low superficial velocities. This discrepancy cannot be fully explained. However, the kind of particles having different electronic and physical properties, such as dielectric loss and particle diameter, which determines voidage among particles are important in determining plasma generation. The voidage among particles is assumed to be particularly important for plasma generation, since plasma was visually observed to form in bubbles, and not in the dense phase.

Thus, in most cases, the fluidization of particles under plasmatic conditions can be dealt with in a manner similar to that for fluidization under non-plasmatic conditions. When the practical temperature of plasma gas in the bed increases sufficiently, fluidization would be kept at gas velocities less than U_{mf}, determined under non-plasmatic conditions [figure 3(a)].

Plasma emission in a fluidized bed

Visual observations indicate that plasma is generated in bubbles. In order to specify the field of plasma generation and its frequency, plasma generation was observed from the following three points, as illustrated in figures 4 and 5: (1) the side of the fluidized bed, to monitor emission in the bed; (2) the surface of the bed; and (3) the side of the freeboard. The results from the latter two points were compared to distinguish emission at the surface of the bed from that in the freeboard. Figures 4 and 5 present time variations in the signal intensity. When Ar was used as the plasma gas, the plasma was hard to generate in the freeboard [figure 4(b)], but pulse-like signals frequently appeared in the fluidized bed [figure 4(c)], indicating plasma generation in the bubbles. Emission was occasionally observed at the surface of the bed, suggesting that part of the plasma that formed in bubbles had penetrated the bed. In the case of H_2 plasma [figure 4(d) and (e)], plasma generated in the fluidized bed in a similar manner, although the signal intensities were, on the whole, lower than those from the Ar plasma. No plasma was found to penetrate the bed. Since the experiments employing Ar and H_2 were carried out with the same value of $U_f - U_{mf}$ (where U_f is superficial velocity), the gas velocities of Ar and H_2 in the bubble phase were likely the same, assuming that gas passed through the dense phase of the bed at the velocity of U_{mf}. The lower signal intensities and lack of plasma penetration through the bed possibly reflected instability of the H_2 plasma compared with the Ar plasma. The frequency of plasma penetrating the bed should depend on the bed height.

Plasma generation in the silicon-fluidized bed behaved differently. The particles were fluidized at the same $U_f - U_{mf}$ as that for the alumina-fluidized bed (figure 5). As shown in figure 5(c), the frequency of Ar plasma generation was smaller than that in the alumina-fluidized bed. By contrast, plasma emission was detected at the surface and in the freeboard, as shown in figure 5(a) and (b). Figure 5(a) presents data from both the surface of the bed and the freeboard, and figure 5(b) presents data regarding the frequency from the plasma emission from the freeboard. Compared with the emission frequency in each figure, the frequency of the plasma emitted at the surface of the bed appeared to be considerable, and was clearly greater than that in the bed. No emission was observed in the freeboard when H_2 plasma was used in the silicon-fluidized bed [figure 5(e)]. The top-view shown in figure 5(d) indicates that plasma emitted at the surface of the bed. The frequency of plasma emission in the bed was much less than that at the surface, indicating that plasma emission occurred exclusively in the vicinity of the surface. The frequency for H_2 plasma was apparently less than that for Ar plasma, further confirming the instability of H_2 plasma.

The differential behavior of plasma generation between alumina- and silicon-fluidized beds is best explained in terms of the physical properties of the particles. The fact that silicon particles significantly absorb microwaves may contribute to the behavioral differences. We believe that this absorbance in the silicon-fluidized bed makes plasma generation difficult, and that plasma generates in bubbles when the bubbles splash at the surface of the bed.

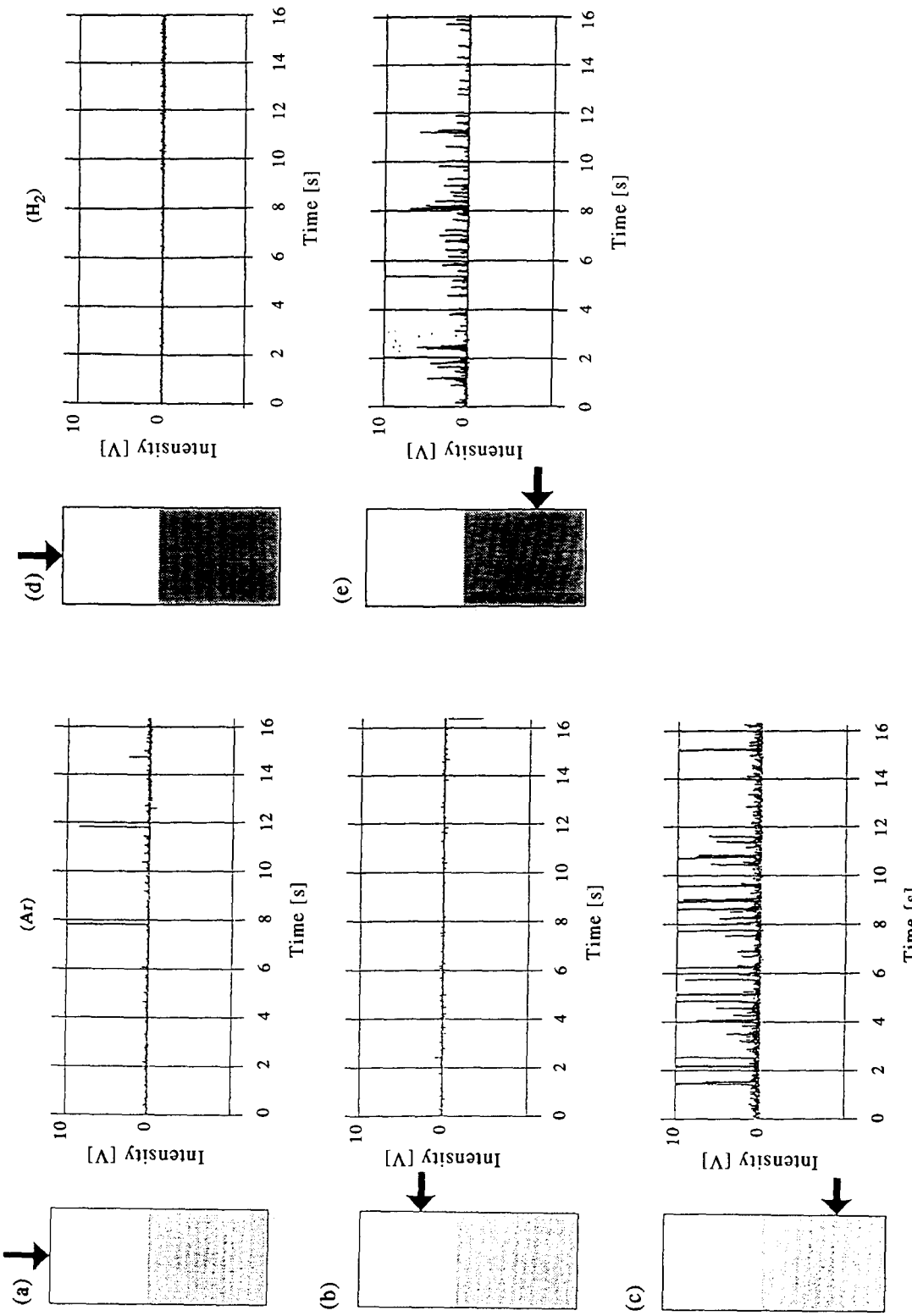

Figure 4. Optical observations of plasma emission for the microwave plasma-fluidized bed of alumina. Fluidization gas: Ar, (a, b, c); H_2, (d, e). Positions and directions for observations are indicated in each figure. $U_f - U_{mf}$, 3.0×10^{-2} m s^{-1}.

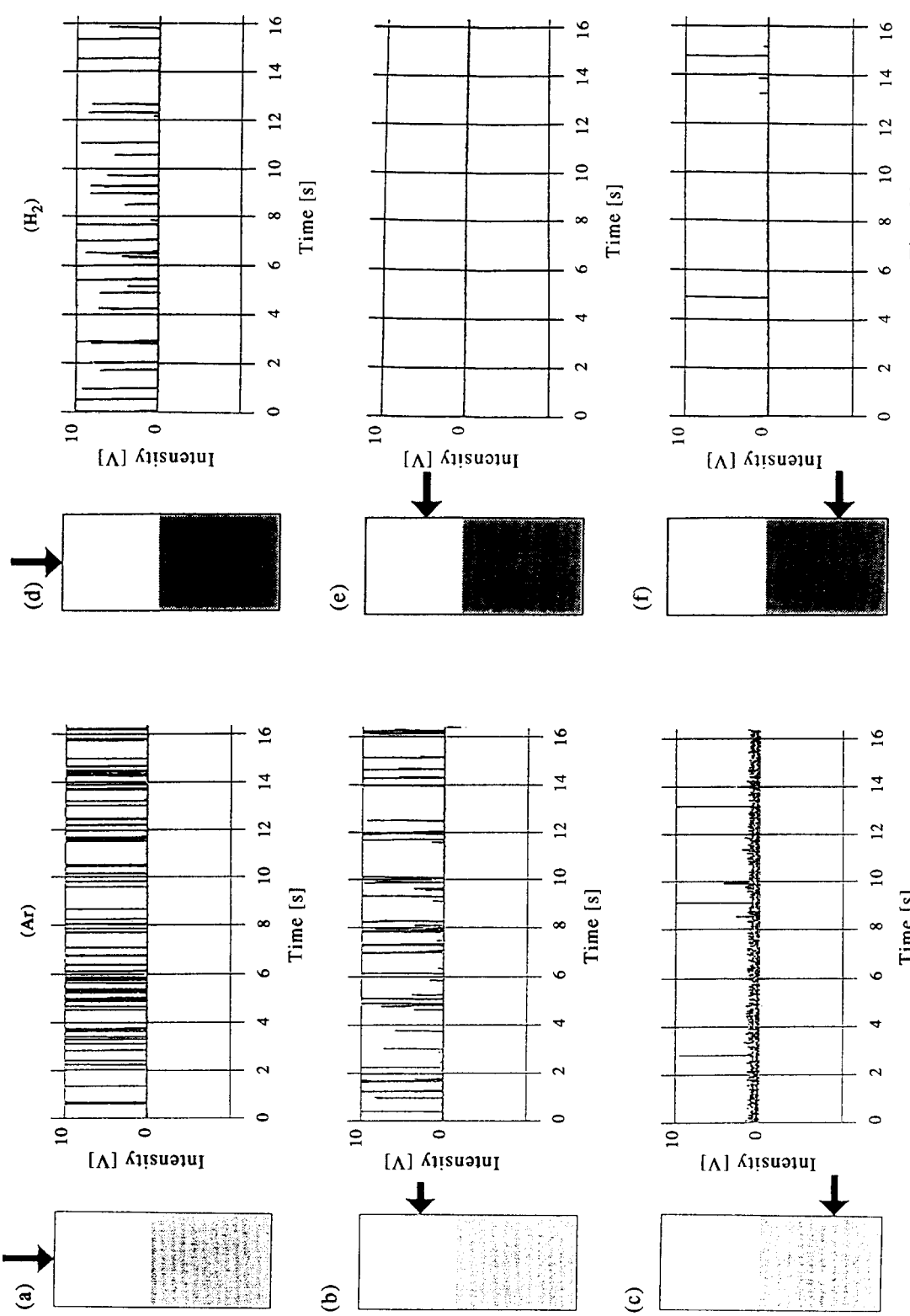

Figure 5. Optical observations of plasma emission for the microwave plasma-fluidized bed of silicon. Fluidization gas: Ar, (a, b, c); H_2, (d, e, f). $U_f - U_{mf}$, 3.0×10^{-2} m s^{-1}.

In order to discuss emission frequency quasi-quantitatively, the frequency was plotted as a function of the superficial velocity of plasma gas (figure 6). Figure 6(a) gives the results for the alumina-fluidized bed. We determined the apparent frequency by using the method that gave the highest frequency among the three methods of counting plasma emission. The lines in figure 6 show the frequency, f, calculated by [3] based on the assumptions that the bubble is spherical, the bubble diameter is constant from the bottom to the surface of the bed, gas superficial velocity in the bubble phase is $U_f - U_{mf}$, and plasma generates in all bubbles.

$$f = A\,(U_f - U_{mf})/V_b \qquad [3]$$

$$A = \pi D^2/4,\ V_b = \pi D_b^3/6$$

where

A = cross-sectional area of reactor (m^2)
V_b = volume of bubble (m^3)
D = inner diameter of reactor (m)
D_b = bubble diameter (m).

The measured emission frequency increased with increasing superficial velocity. The straight line calculated on the assumption of $D_b = 0.5D$ was in good agreement with the experimental values. Thus, it is likely that Ar plasma generated in all bubbles with $D_b = 0.5D$, which strongly supports our conclusion that plasma is hard to generate in the dense phase, since the intercept of the line to the abscissa represents U_{mf}. When H_2 was employed as the plasma gas, the frequency also increased linearly with increasing superficial velocity. The line obtained by the calculation on the assumption of $D_b = 0.8D$ was in agreement with the experimental data.

By contrast, a linear relation between the emission frequency and the superficial velocity was not obtained for the silicon-fluidized bed. In the case of the Ar–silicon system shown in figure 6(b), the experimental data were scattered around the line corresponding to $D_b = 0.8D$, but the emission frequency appeared nearly constant at 0.8 s^{-1}. The emission frequency measured for the Ar–silicon system was much less than that for the Ar–alumina system (see optical observation results, figures 4 and 5), indicating that plasma was difficult to generate in the silicon-fluidized bed. We concluded that the results shown in figure 6(b) were due to the difficulty of plasma generation, i.e. plasma

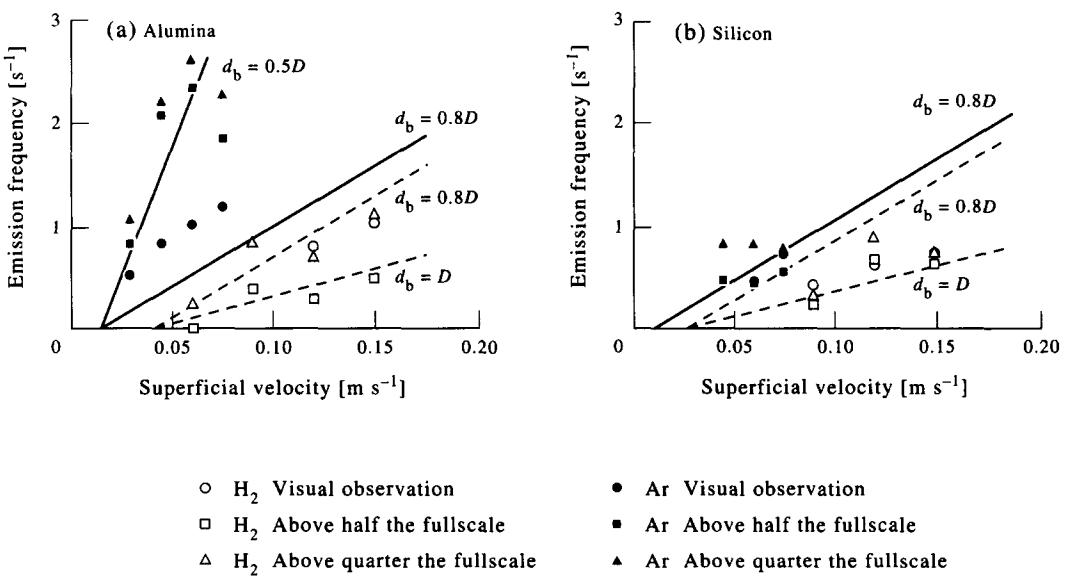

Figure 6. Relation between superficial velocity and the frequency of plasma emission observed from the side of the bed. Two kinds of gases, Ar and H_2, were used: solid line, Ar; dotted line, H_2. $U_f - U_{mf}$ was 3.0×10^{-2} m s^{-1}. Emission frequency in a given period was determined in three ways: (1) the number of plasma emissions was visually counted; (2) the number of plasma emissions giving intensities greater than 5 V, half the full-scale on the recording chart, was counted; and (3) the number of plasma emissions giving intensities greater than 2.5 V, one quarter of the full-scale on the recording chart, was counted. The recording chart refers to figures 4 and 5. Straight lines show the frequencies calculated by [3].

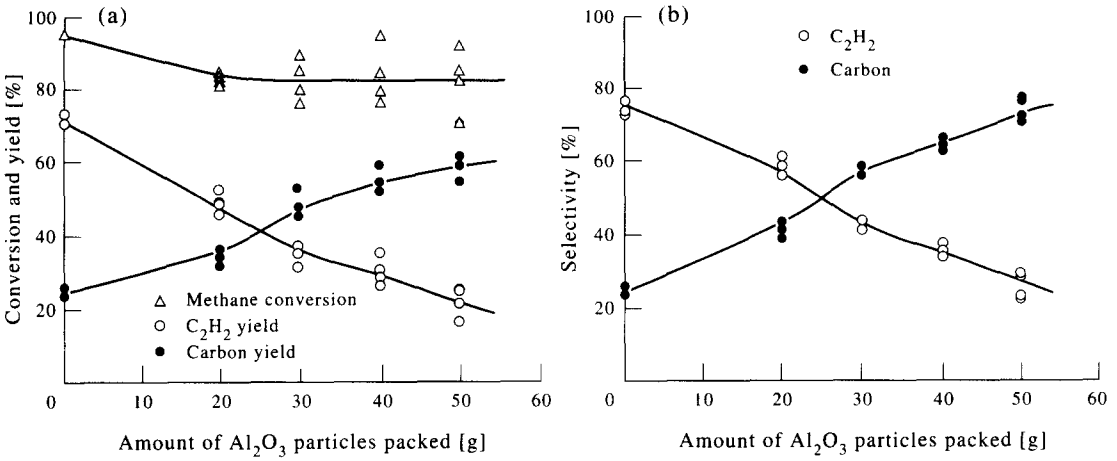

Figure 7. Effect of the amount of alumina particles on (a) the level of methane conversion and product yields and (b) the selectivities. The amount of alumina packed was 50 g. The superficial velocity of the reaction gas mixture was 6.0×10^{-2} m s^{-1} ($U_{mf} = 3.2 \times 10^{-2}$ m s^{-1}).

generated in part of the bubbles. It appears that the emission frequency in the silicon-fluidized bed was determined by the power of the microwaves. The results for the H_2–silicon system are shown in figure 6(b). A similar analysis can be made for the plasma generation.

Methane conversion in the plasma-fluidized bed reactor

We attempted to develop a new method of particle processing, such as coating and surface treatment, by using a fluidized bed. If plasma generates in bubbles and freeboard resulting in an excitation of reactive gases there, then particle processing in this type of reactor would be difficult to achieve. We carried out CH_4 conversion in the alumina-fluidized bed, in which plasma generated well in bubbles, in order to confirm the occurrence of a heterogeneous reaction giving deposits on particle surfaces.

Figure 7 presents the results of CH_4 conversion as a function of the amount of alumina packed. The data plotted at 0 g of alumina packed represent the results in an empty reactor. The level of CH_4 conversion slightly decreased from 97% to about 80% with the presence of alumina particles. However, the amount of alumina packed hardly affected the conversion level. On the other hand, the yield of C_2H_2 decreased and that of carbon increased as the amount of alumina increased. The selectivity to carbon was dramatically increased, from 25 to 75%, by a particle loading of 50 g. It is noteworthy that the carbon yield increased as the amount of alumina increased, whereas CH_4 conversion was decreased by the particles compared with that in an empty reactor. This is conclusive evidence for the occurrence of heterogeneous deposition on the surface of alumina in the microwave plasma-fluidized bed reactor. Since the bed temperature, which was close to the temperature of the particles, was around 400 K, CH_4 could not decompose thermally. Thus, the CH_4 was excited by the plasma generating in the bubbles, the excited species entered into the dense phase by gaseous exchange between the dense phase and the bubbles, and carbon deposition occurred on the surface of the particles heterogeneously. The possibilities for using this type of reactor for a new method of particle processing appear good. We are currently investigating the effect of reaction conditions on the progress of methane conversion, and the morphological and structural features of the carbon deposits.

4. CONCLUSIONS

A microwave plasma-fluidized bed was developed as a novel method of particle processing. The hydrodynamics of the plasma-fluidized bed reactor depend significantly on the physical properties of the particles, such as diameter and dielectric loss.

In the alumina-fluidized bed reactor, plasma generates in most of the bubbles, but not in the dense phase, and part of the plasma in the bubbles penetrates the bed. In the silicon-fluidized bed

reactor, by contrast, plasma is difficult to generate, even in the bed, and generates at the surface of the bed where the bubbles splash. Plasma also frequently generates in the freeboard.

The methane conversion in the alumina-fluidized bed described above indicates that this new type of plasma reactor will allow a novel method of particle coating via heterogeneous CVD.

Acknowledgement—We wish to express our appreciation for Grants-in-Aid for Scientific Researchers by the Ministry of Education, Science and Culture, Japan.

REFERENCES

FLAMANT, G. 1990 Hydrodynamics and heat transfer in a plasma spouted bed reactor. *Plasma Chem. Plasma Proc.* **10,** 71–85.

JUREWICZ, J., PROULX, P. & BOULOS, M. 1985 The plasma spouted bed reactor. *Proc. of 7th Int. Symp. on Plasma Chem.*, Eindhoven, p. 243.

KOJIMA, T., MATSUKATA, M., ARAO, M., NAKAMURA, M. & MITSUYOSHI, Y. 1991 Development of a plasma jetting fluidized bed reactor. *J. Phys. II* **C2,** 429–436.

MATSUKATA, M., OH-HASHI, H., KOJIMA, T., MISTUYOSHI, Y. & UEYAMA, K. 1992 Vertical progress of methane conversion in a d.c. plasma jetting fluidized bed reactor. *Chem. Engng Sci.* **47,** 2963–2968.

ROGERS, T. & MORIN, T. J. 1991 Slip flow in fixed and fluidized bed plasma reactors. *Plasma Chem. Plasma Proc.* **11,** 203–228.

WIERENGA, C. R. & MORIN T. J. 1989 Characterization of a fluidized-bed plasma reactor. *AlChE Jl* **35,** 1555–1558.